INFLUENCE OF EXTERNAL TOROIDAL FLUX ON LOW-ASPECT-RATIO TOROIDAL PLASMA

S. IKUNO and M. NATORI
Institute of Information Sciences and Electronics,
University of Tsukuba,
Tennoudai 1-1-1, Tsukuba, Ibaraki 305-8573, Japan

A. KAMITANI
Department of Electrical and Information Engineering,
Faculty of Engineering, Yamagata University,
Johnan 4-3-16, Yonezawa, Yamagata 992-8510, Japan

Abstract

In the HIST device, the external flux is generated by two kinds of currents: the current I_s flowing along the symmetry axis and the bias coil current I_D. The influence of the external flux on the MHD equilibrium and stability of the low-aspect-ratio toroidal plasma in the HIST device is investigated numerically. Equilibrium configurations of the low-aspect-ratio toroidal plasma in the HIST device are numerically determined by means of the combination of FDM and BEM. The influence of I_s and I_D on their stability is also investigated by using the Mercier criterion. The results of computations show that the Mercier limit decreases to zero with increasing I_s and with decreasing I_D. Moreover, either a further increase in I_s or a further decrease in I_D raises the Mercier limit considerably. Besides, the equilibrium configuration in the HIST device changes its state from spheromak through ultra-low q to tokamak with increasing I_s and with decreasing I_D.

1. INTRODUCTION

Recently, the low-aspect-ratio toroidal plasma has attracted great attention as a new concept of the fusion device. It has some advantages that is not found in the tokamak: large elongation, high beta ratio, large plasma current and simplicity of the metallic vessel. However, it has not been clear whether the scaling law of the general large-aspect-ratio tokamak is applicable to the low-aspect-ratio toroidal plasma or not. For this reason, intensive studies on the low-aspect-ratio toroidal plasma have been performed theoretically [1] and experimentally [2, 3]. At Himeji Institute of Technology, the low-aspect-ratio toroidal plasma has been formed and sustained successfully in the HIST device [2, 3].

In the HIST device, the Marshall gun is used for the formation of the plasma. After formed in the gun, the plasma is injected into the flux conserver (FC) and it forms an equilibrium configuration there. In order to supply the plasma with the toroidal flux, the center conductor is inserted along the symmetry axis and the electric current is applied along it. Furthermore, the DC helicity injection method is utilized for driving the plasma current externally.

The purpose of the present study is to numerically determine realistic MHD equilibria in the HIST device and to investigate the influence of the external flux on their Mercier limit.

2. MHD EQUILIBRIUM CONFIGURATION

In the HIST device, the spherical FC of radius 500mm is joined to the helicity injector. The bias coil of rectangular cross section is placed in the helicity injector and is covered with the shielding wall so that the plasma may not be in contact with the coil. Moreover, the center conductor of radius 57mm is inserted along the symmetry axis in order to apply the current I_s along it. In Fig.1, we show the model of the FC and the helicity injector which is used in the present study. In the following, the region in

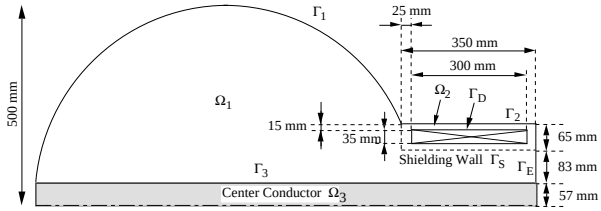

FIG. 1 The model of the FC and the helicity injector.

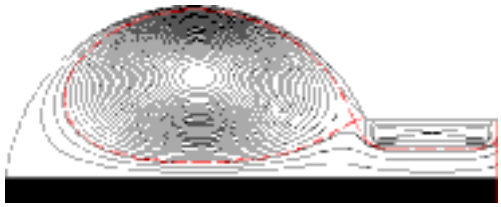

FIG. 2 The equilibrium configuration for the case with $\varepsilon = 0.0$, $\sigma = 0.1$, $\delta = 0.03$, $I_s/I_p = 0.15$ and $I_D/I_p = 0.50$.

which equilibrium configurations are determined is divided into three subregions, Ω_1, Ω_2 and Ω_3.

In the HIST experiment, the bias coil is turned on long before the plasma is ejected from the Marshall gun. By taking this fact into account, we assume that the bias flux extends all over the space when the equilibrium formation has been finished. Moreover, the life time of the plasma is enough long as compared with the skin time of the shielding wall, whereas it is sufficiently shorter than that of the FC wall and the center conductor. Therefore, we can assume that the magnetic flux generated by the plasma current penetrates inside the shielding wall and that it does not penetrate outside the FC. In addition, if the plasma moves on the field lines intersecting the shielding wall, it will be cooled due to the thermal conduction along the lines. For this reason, we also assume that the plasma exists only on the field lines which does not intersect to the shielding wall.

Let us use the cylindrical coordinate system (z, r, φ) and take the symmetry axis as z-axis. Since the equilibrium configuration of the low-aspect-ratio toroidal plasma is axially symmetrical, we can determine it by solving the Grad-Shafranov equation in (z, r) plane. Under the above assumptions, the Grad-Shafranov equation can be written in the form,

$$-\hat{L}\psi = \chi_{\Omega_1}(z, r)\left(\mu_0 r^2 \frac{\mathrm{d}p}{\mathrm{d}\psi} + \frac{{\mu_0}^2}{2}\frac{\mathrm{d}I^2}{\mathrm{d}\psi}\right) . \tag{1}$$

Here ψ and μ_0 denote a magnetic flux function and a magnetic permeability of vacuum, respectively. Furthermore, $\hat{L}$ denotes the Grad-Shafranov operator and $\chi_{\Omega_1}(z, r)$ represents the characteristic function defined by

$$\chi_{\Omega_1}(z, r) \equiv \begin{cases} 1; & (z, r) \in \Omega_1 \\ 0; & (z, r) \notin \Omega_1 \end{cases} , \tag{2}$$

Besides, $p(\psi)$ and $I(\psi)$ denote the plasma pressure and the toroidal magnetic field function, respectively. In order to satisfy the above assumptions, we employ the following functions as $I(\psi)$ and $p(\psi)$:

$$I(\psi) = \frac{\lambda}{\mu_0 L}(\psi_{\mathrm{axis}} - \psi_{\mathrm{S}})\Theta(\Psi)[\sqrt{\Psi^2 + \delta^2}(1 + \sigma\Psi) - \delta^2\sigma\log\left(\Psi + \sqrt{\Psi^2 + \delta^2}\right) - \delta + \delta^2\sigma\log\delta] + \frac{I_{\mathrm{s}}}{2\pi} , \tag{3}$$

$$\frac{\mathrm{d}p}{\mathrm{d}\psi} = \frac{\varepsilon}{\mu_0 L^4}(\psi_{\mathrm{axis}} - \psi_{\mathrm{S}})(1 - \Psi)\,\Theta(\Psi)\,S(\Psi) . \tag{4}$$

Here, λ, σ, δ and ε are constants and L represents a radius of the FC. The function $S(x)$ in Eq. (4) is defined by $S(x) \equiv x / \sqrt{\delta^2 + x^2}$ and $\Theta(x)$ denotes Heaviside's step function. Besides, ψ_{axis} and ψ_{s} denote the values of ψ on the magnetic axis and on the plasma surface, respectively, and Ψ is defined by $\Psi \equiv (\psi - \psi_{\mathrm{s}})/(\psi_{\mathrm{axis}} - \psi_{\mathrm{s}})$. The plasma surface $\psi = \psi_{\mathrm{s}}$ is determined so that the plasma may exist inside the

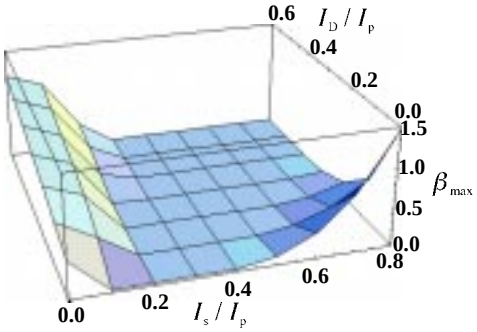

FIG. 3 The Mercier limit β_{max} as functions of I_s/I_p and I_D/I_p for the case with $\sigma = 0.1$ and $\delta = 0.03$.

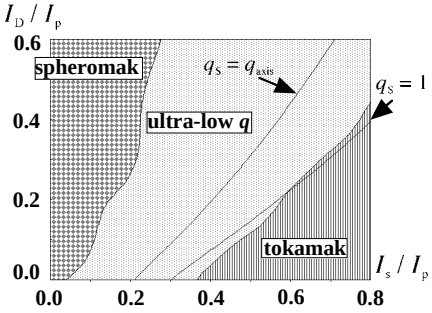

FIG. 4 The classification of the equilibrium configurations with the Mercier limit for the case with $\sigma = 0.1$ and $\delta = 0.03$.

most outer closed magnetic surface. If the X point appears in Ω_1, the value of ψ on the separatrix is chosen as ψ_s. On the other hand, the maximum of ψ on Γ_s is adopted as ψ_s if the X point does not exist in Ω_1. Now let us consider the boundary conditions to Eq. (1). Since the bias flux extends all over the space, we set $\psi = \psi_D$ on Γ_1, Γ_2, Γ_3 and Γ_E. Here ψ_D denotes the bias flux produced by the bias coil current I_D. On the surface Γ_D of the bias coil, ψ is an unknown constant and its normal derivative satisfies

$$\oint_{\Gamma_D} \frac{1}{r}\frac{\partial \psi}{\partial n} \mathrm{d}\ell = I_D \ . \tag{5}$$

Equation (1) and the boundary conditions have six parameters, λ, σ, ε, δ, I_s/I_p and I_D/I_p. Here, I_p denotes a total plasma current. Once a set of σ, ε, δ, I_s/I_p and I_D/I_p is given, Eq. (1) and its associated boundary conditions constitute a nonlinear eigenvalue problem with an eigenvalue λ. After the linearization of Eq. (1), the problem is solved by use of the iterative method. However, the linearized equation is composed of both the homogeneous and the inhomogeneous equation because of the characteristic function in Eq. (1). Thus, it is difficult to express the interface condition precisely. In order to overcome these difficulties, we solve the equation numerically by means of the combination of FDM and BEM [4]. By using the above method, the equilibrium configuration in the HIST device can be determined. A typical example is shown in Fig. 2.

3. MHD STABILITY

In Fig. 3, we show the dependence of the Mercier limit β_{max} on I_s/I_p and I_D/I_p. As the definition of the beta ratio, its value on the magnetic axis is adopted. We see from this figure that β_{max} decreases to zero with an increase in I_s/I_p and with a decrease in I_D/I_p, and that either a further increase in I_s/I_p or a further decrease in I_D/I_p will raise β_{max} considerably. In order to explain such a behavior of β_{max}, let us introduce the quantity S defined by

$$S \equiv \underset{0 \le \Psi \le 1}{\mathrm{Max}} \left(\frac{\mathrm{d}q}{\mathrm{d}\Psi} \right) \cdot \underset{0 \le \Psi \le 1}{\mathrm{Min}} \left(\frac{\mathrm{d}q}{\mathrm{d}\Psi} \right) \ . \tag{6}$$

In case of $S > 0$, the equilibrium configuration with $q_{axis} > q_S$ and that with $q_{axis} < q_S$ correspond to a spheromak and a tokamak configuration, respectively. Here, q_{axis} and q_S denote the values of the safety factor on the magnetic axis and on the plasma surface, respectively. In case of $S < 0$, a pitch minimum region exists between the plasma surface and the magnetic axis and, therefore, the equilibrium configuration corresponds to an ultra-low-q configuration in this case. In Fig. 4, we show the classification of equilibrium configurations with the Mercier limit. Furthermore, the dependence of q_{axis} and q_S on I_s/I_p and I_D/I_p is shown in Fig. 5. The values of q_{axis} and q_S increase monotonously with increasing I_s/I_p and

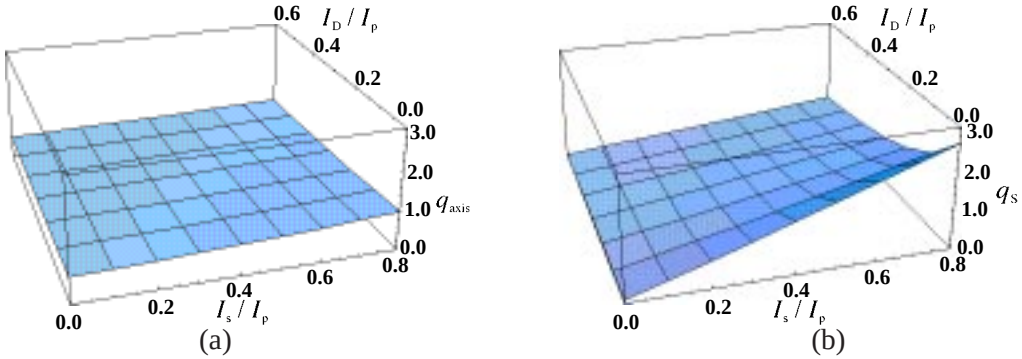

FIG. 5 The values of (a) q_{axis} and (b) q_S as functions of I_s/I_p and I_D/I_p for the equilibrium configurations with the Mercier limit for the case with $\sigma = 0.1$ and $\delta = 0.03$.

with decreasing I_D/I_p. In addition, the increasing tendency of q_S is more remarkable than that of q_{axis}. This fact indicates that the stabilization effect by the magnetic shear becomes weak near the plasma surface until the pitch minimum region appears between the plasma surface and the magnetic axis. This is why the equilibrium configuration changes its state from the spheromak to the ultra-low-q configuration with increasing I_s/I_p and with decreasing I_D/I_p. Incidentally, the ultra-low-q configuration becomes unstable against localized perturbations because of the existence of the pitch minimum region. Either a further increase in I_s/I_p or a further decrease in I_D/I_p will remove the pitch minimum region and will enhance the shear stabilization effect near the plasma surface. Consequently, the configuration changes its state from the ultra-low-q to the tokamak configuration. From these results, we can conclude that the appearance and the disappearance of the pitch minimum region are closely related to the behavior of β_{max}.

As is well known, the plasma is stable against the $n = 1$ internal kink mode if the mode rational surface with $q = 1$ does not exist between the magnetic axis and the plasma surface. Since the inequality $q_{axis} < 1$ is fulfilled throughout the present analysis, we might conclude that the Mercier limit equals to the beta limit for the case with $q_S < 1$ [5, 6].

4. CONCLUSIONS

We have determined equilibrium configurations of the low-aspect-ratio toroidal plasma in the HIST device numerically and have investigated the influence of I_s and I_D on their stability. Conclusions obtained in the present study are summarized as follows. 1) The values of q_{axis} and q_S increase monotonously with increasing I_s/I_p and with decreasing I_D/I_p. In addition, the increasing tendency of q_S is more remarkable than that of q_{axis}. This fact leads to the appearance and the disappearance of the pitch minimum region. 2) The value of β_{max} decreases to zero with an increase in I_s/I_p and with a decrease in I_D/I_p, and either a further increase in I_s/I_p or a further decrease in I_D/I_p will raise β_{max} considerably. Such a behavior of β_{max} can be explained from the standpoint of the shear stabilization near the plasma surface. 3) The low-aspect-ratio toroidal plasma in the HIST device is classified into three types of configurations: spheromak, ultra-low q and tokamak.

REFERENCES

[1] BROWNING, P. K., *et al.*, Plasma Phys., Control. Fusion **35** (1993) 1563-1583.
[2] NAGATA, M., *et al.*, Proc. Int. Conf. on Plasma Phys. Vol. 2(1996) 1210-1213.
[3] NAGATA, M., *et al.*, Proc. US-Japan Workshop on the Spherical Torus and Low Aspect Ratio Tokamaks, Vol. 2(1996) 717-730.
[4] KAMITANI, A., *et al.*, Periodica Polytechnica Ser. El. Eng. **38** (1994) 257-266.
[5] GAUTIER, P., *et al.*, Nucl. Fusion **21** (1981) 1399-1407.
[6] KAMITANI, A., *et al.*, J. Phys. Soc. Jpn. **60** (1991) 512-517.